Eur. Phys. J. B (2015) 88: 277
DOI: 10.1140/epjb/e2015-60460-3

THE EUROPEAN PHYSICAL JOURNAL B

Regular Article

Preparation and dielectric properties of the lead-free $BaFe_{1/2}Nb_{1/2}O_3$ ceramics obtained from mechanically triggered powder*

Dariusz Bochenek[1,a], Przemysław Niemiec[1], Izabela Szafraniak-Wiza[2], Małgorzata Adamczyk[1], and Ryszard Skulski[1]

[1] University of Silesia, Institute of Technology and Mechatronics, 12, Żytnia St., 41-200 Sosnowiec, Poland
[2] Poznan University of Technology, Institute of Material Science and Engineering, 5, M.Skłodowskiej-Curie Sq., 60-965 Poznań, Poland

Received 11 June 2015 / Received in final form 24 July 2015
Published online 26 October 2015

Abstract. In the paper the influence of mechanical activation of the powder on the final dielectric properties lead-free $Ba(Fe_{1/2}Nb_{1/2})O_3$ (BFN) ceramic was examined. The BFN ceramics were obtained by 3-steps route. Firstly, the substrates were pre-homogenized in a planetary ball mill. Than, the powder was activated in vibratory mill (the shaker type SPEX 8000 Mixer Mill) for different duration between 25 h and 100 h. The influence of the milling time on the BFN powder was monitored by X-ray diffraction. The diffraction data confirmed that the milling process of the starting components is accompanied by partial synthesis of the BFN materials. The longer of the high-energy milling duration the powders results in increasing the amount of amorphous/nanocrystalline content. The mechanically activated materials were sintered in order to obtain the ceramic samples. During this temperature treatment the final crystallisation of the powder appeared what was confirmed by XRD studies. The performed dielectric measurements have revealed the reduction of the dielectric loss of the BFN ceramics compared to materials obtained by classic methods.

1 Introduction

Perovskite ceramics of a general formula ABO_3 are widely used in various modern microelectronics and micromechatronic devices such as microwave frequency resonators, multilayer capacitors, sensors, detectors and actuators [1–3]. The most popular material for such applications (esp. for high performance piezoelectric applications) is based upon lead-based composition with $Pb(Zr_{1-x}Ti_x)O_3$ (PZT) [4]. Recently worldwide environmental considerations and several national regulations (e.g. EC directives) are demanding the elimination of lead-based materials from all the consumer items [5,6]. This has created urgency for finding alternative to PZT [7]. One of possible candidate to replace lead-contained ceramics is $BaFe_{1/2}Nb_{1/2}O_3$ (BFN), which exhibit typical relaxor ferroelectric behaviour characterized by a broad dielectric transition with frequency dependent [8,9]. The extensive research has shown that the ceramic BFN material has the very high dielectric permittivity [10,11] but with very high values of dielectric losses, too.

This work was focused on investigating the influences of mechanical activation on the final properties of lead-free $Ba(Fe_{1/2}Nb_{1/2})O_3$ (BFN) ceramics.

2 Experiment

As starting components for the synthesis of BFN, the high purity powders have been chosen: iron oxide Fe_2O_3 (>99%), niobium oxide Nb_2O_5 (99.99%) and barium carbonate $BaCO_3$ (99.99%). Stoichiometric amount of the starting powders were weighed according to the reaction: $BaO + 0.25Fe_2O_3 + 0.25Nb_2O_5 \rightarrow BaFe_{1/2}Nb_{1/2}O_3$ and pre-homogenized in a Fritsch-type planetary ball mill for 8 h (wet in ethyl alcohol).

The dried mixture was mechanically activated by ball-milling method. The mechanical milling was carried out in a SPEX 8000 Mixer Mill in the air atmosphere and at room temperature. The powder was loaded into stainless steel vial with stainless steel balls. The ball to powder weight ratio (BPR) parameter was 5:1. The mill was running for different periods between 25 h and 100 h for powder preparation. The milling process was controlled by X-ray diffraction studies at various times of mechanical activation. XRD measurements were performed

* Contribution to the Topical Issue "Materials for Dielectric Applications", edited by Maciej Jaroszewski and Sabu Thomas.

[a] e-mail: dariusz.bochenek@us.edu.pl

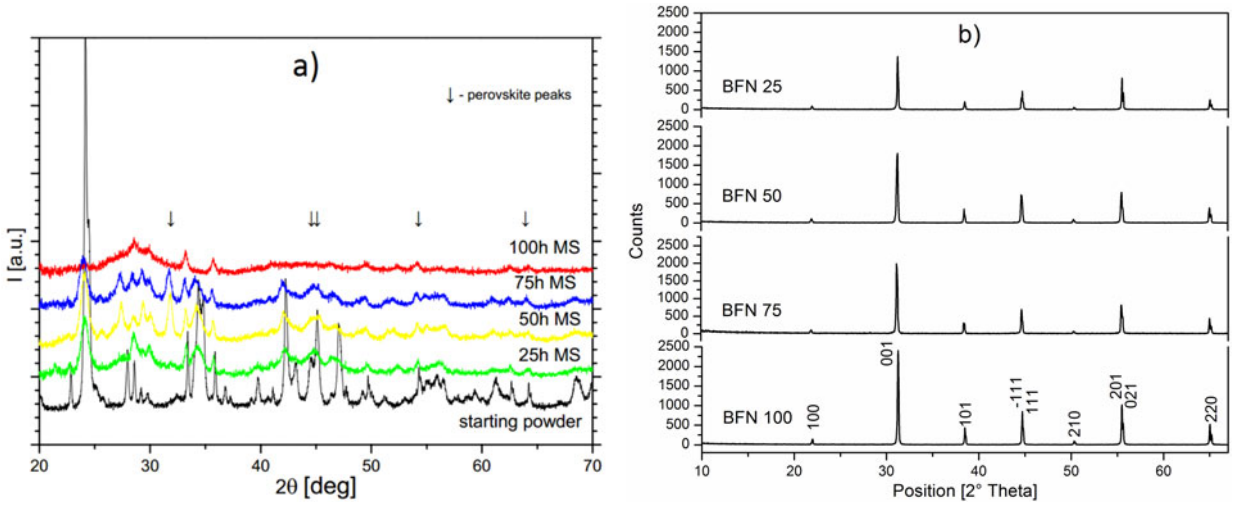

Fig. 1. X-ray patterns: (a) of the BFN powders after different stages of mechanical activation, (b) of the BFN ceramics prepared from mechanical activated powders.

with PANalytical Empyrean X-ray powder diffractometer ($Cu_{K\alpha}$ radiation, 45 kV, 40 mA).

Pre-synthesized (by high-energy milling) BFN powders were calcined. The calcination was done at temperature 1250 °C for 4 h for several samples obtained after different milling durations. Finally the calcined powders were pressed and sintered by free-sintering methods under the following conditions: $T_s = 1350$ °C/$t_s = 4$ h. The final crystallographic structures of obtained ceramic samples were investigated by X-ray measurements at room temperature with the diffractometer Phillips X'Pert APD (with a Cu lamp and graphite monochromator) in the angular 2 from 12° to 62° (step 0.02° and measurement time 4 s/step). The microstructure of ceramics was examined by scanning electron microscope (SEM) HITACHI S-4700. The stoichiometry of samples was confirmed by electron dispersive spectroscopy (EDS) analysis. Dielectric measurements were performed using the Precision LCR Meter QuadTech 1920 during the heating cycle (from room temperature to 380 °C) in the frequency range from 20 Hz to 20 kHz of the measuring field.

Measurements of direct current electrical conductivity were carried out in the range from 20 °C to 310 °C using a 6517B Keithley electrometer.

3 Results and discussion

The XRD patterns of the starting (pre-homogenized) and mechanically activated powders are shown in Figure 1. The results of XRD studies have pointed at the mechanical activation of the initial reaction (occurring) between the starting components. As the result several intermediate phases have been formed and the perovskite traces have been also recorded.

The presented results show an increase in the share of the amorphous part of the powder's volume with duration of the high-energy milling; this is in agreement with the results concerned the mechanical syntheses of other perovskite [12–14].

Table 1. Influence of the high-energy milling on the properties of the BFN ceramics (heating cycle).

	BFN25	BFN50	BFN75	BFN100
Time mechanical activation	25 h	50 h	75 h	100 h
ρ_{eksp}[g/cm^3]	5.963	6.062	6.116	6.156
T_m [°C]	286	275	280	282
ε_r	46 470	42 350	23 740	33 050
tanδ at T_r	1.05	0.67	0.60	0.44
ε_m	106 470	145 250	127 750	99 400
E_{Act} [eV] in I	0.39	0.41	0.35	0.34
E_{Act} [eV] in II	0.80	0.76	0.81	0.79
τ_0 [s] $\times 10^7$	9.19	6.15	7.68	13.19

Moreover the X-ray investigations of ceramic samples showed that additional annealing lead to complete reaction and the full synthesis of BFN powders. On diffraction patterns are visible only the lines connected with the perovskite structure without any detectable lines of secondary phase (Fig. 1b). The X-ray data were used to calculate parameter of unit cell. The BFN ceramics is characterized by monoclinic structure. The lattice parameters obtained from X-ray patterns were: $a = 4.0743$ Å, $b = 4.0388$ Å, $c = 2.8759$ Å (the best fit was obtained for the pattern ICSD No.00-057-0771 [15]).

The microstructure of the BFN ceramics exhibits a compact structure of densely packed grains. For shorter milling time the grain size is non homogenous. The average grain size of the final ceramic sample decreases with increasing the mechanical activation time (Fig. 2), however the number of defects in the grains increases. As the results the packing density and density of ceramics increase (Tab. 1), greatly reducing its porosity. The density has increased between 5.96 g/cm^3 (for BFN25) and 6.16 g/cm^3

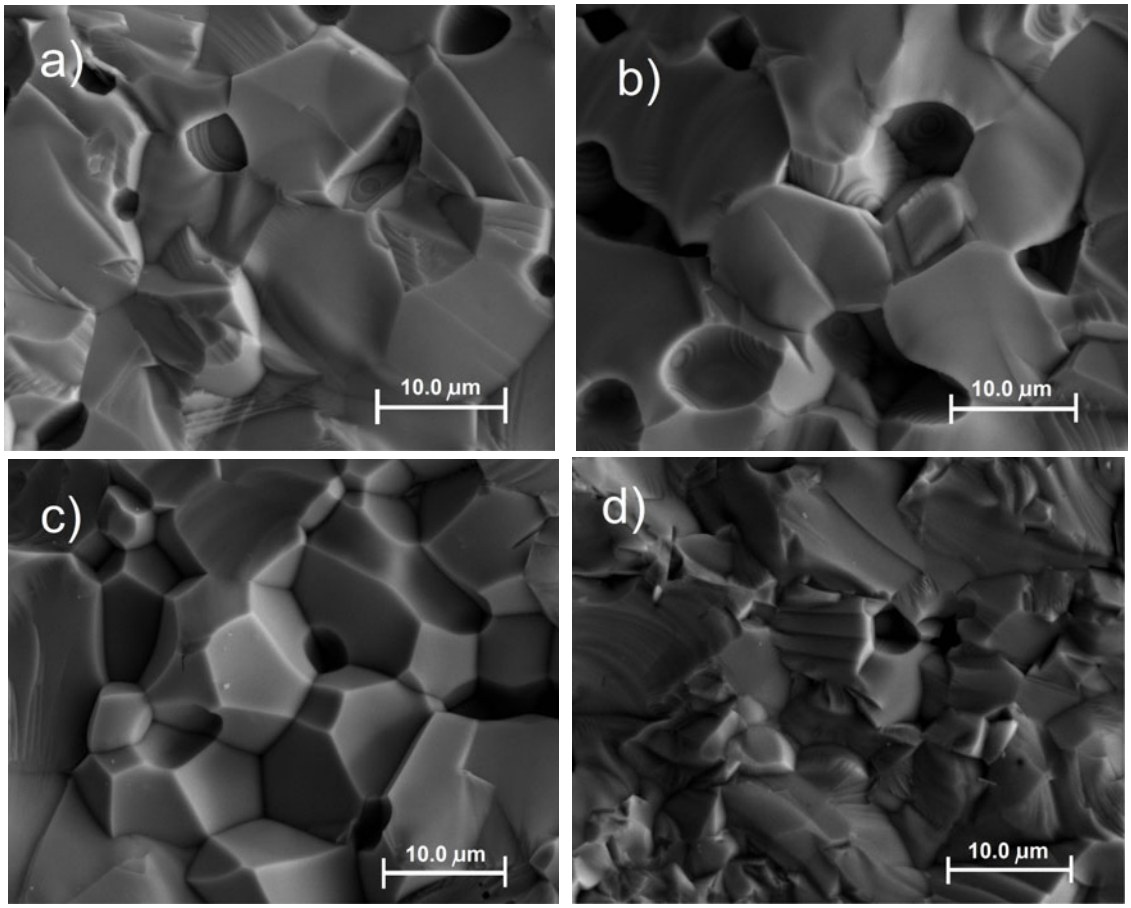

Fig. 2. SEM images of the microstructures BFN ceramics obtained from (a) 25 h, (b) 50 h, (c) 75 h, (d) 100 h high-energy milled powders.

(for BFN100) what is 91.2% and 94.1% of the theoretical value, respectively. In the case of the BFN25, BFN50 and BFN75 samples fracture occurs mainly in the grain boundary, which shows a higher strength compared to the grain boundaries of the grain (less amorphous). If the grain size is increased, fracture toughness of ceramics is slightly increased. In case of the BFN100 sample high defected degree after prolonged milling causes weakness ceramic grains, which results in cracking through the grain (Fig. 2d).

The EDS analysis was carried out on the ten randomly selected areas of the fracture surface of all discussed samples. Investigations confirmed that the milling process has no influence on stoichiometry of the ceramics (Fig. 3).

In a number of papers including dielectric studies of the BFN ceramics, the authors have presented high values of dielectric permittivity, but on temperature dependences of dielectric permittivity $\varepsilon(T)$ no clear ferroelectric-paraelectric phase transition or other phase transition could be observed at all [16–18]. In order to clear the comparison results of the obtained sample test results ε (T) are shown for 1 kHz.

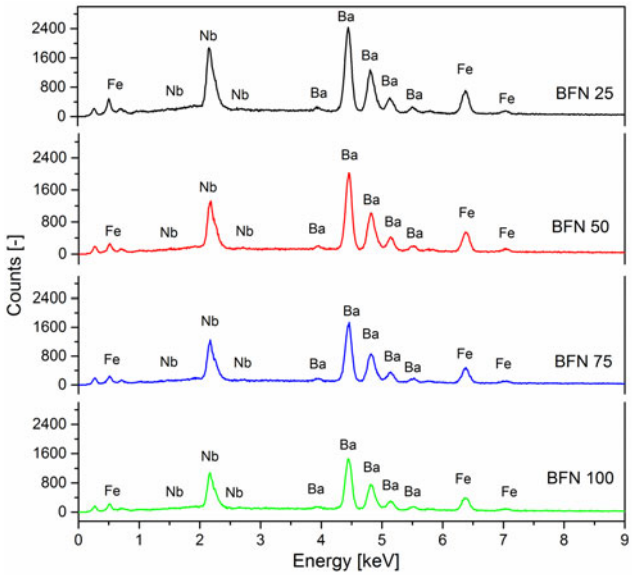

Fig. 3. EDS images of the BFN ceramics.

The temperature dependences of ε (T) for the BFN ceramics (Fig. 4a) exhibit broad maximum at T_m temperature, which is probably connected with the phase transition from ferroelectric phase to paraelectric ones. The reason for maximum broadening is consequence of distribution's disorder of B-side ions (Fe, Nb) in the perovskite

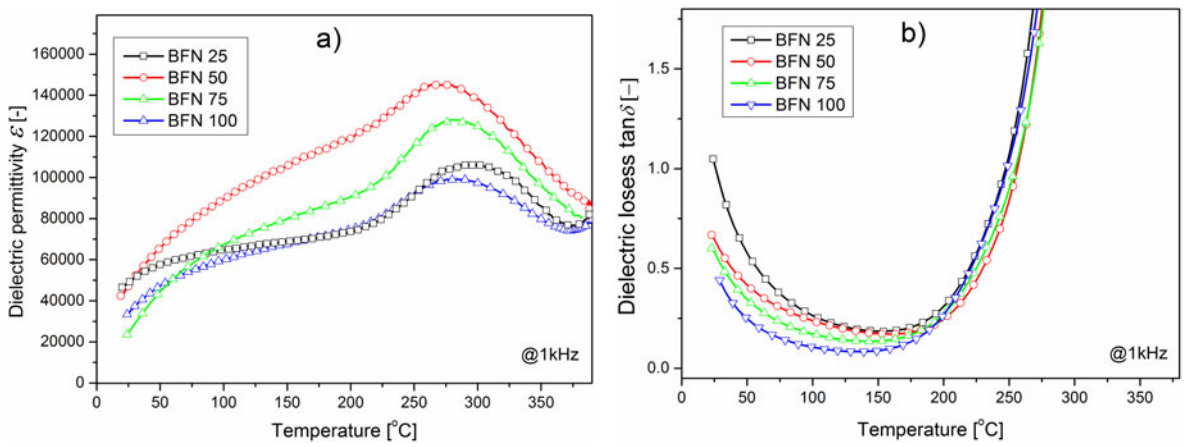

Fig. 4. Influence of the high-energy milling time on (a) ε (T) and (b) tanδ (T) for the BFN ceramics ($\nu = 1$ kHz).

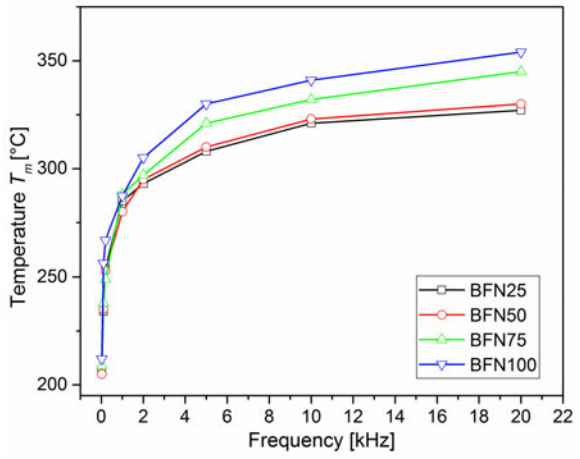

Fig. 5. Influence of the high-energy milling time on the phase transition temperature (T_m).

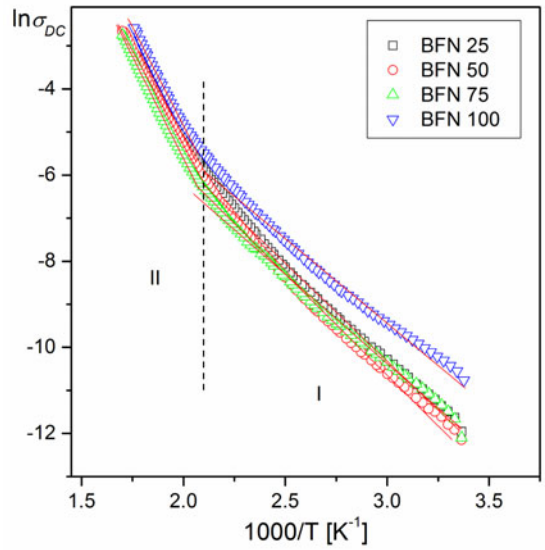

Fig. 6. The ln$\sigma_{DC}(1/T)$ relationship for the BFN ceramics.

unit cell. This may lead to the appearance of compositional fluctuations and conduct to different local Curie temperatures in the different regions of ceramics. This causes broadening phase transition in BFN ceramic samples. The value of dielectric permittivity, especially at the maximum ε_m, is high in a very wide temperature range for all samples. Moreover the discussed maximum of dielectric permittivity has the large value especially for the BFN50 and the BFN75 samples.

The B-side ions (Fe, Nb) disorder, mentioned above, is also responsible for the strong ferroelectric relaxor behaviour revealed by those ceramics [9,17]. Namely magnitude of the dielectric permittivity decreases with increasing frequency of measuring field and the maximum shift to higher temperatures. The dispersion of T_m temperature is strongly dependent on the duration time of the mechanical activation – prolongation of activation time results in an increase in the dispersion. The effect of the high-energy milling time on the degree of the frequency dispersion (defined here as the difference between the T_m measured at 20 Hz and that measured at 20 kHz) is the following: 121° for BFN25, 125° for BFN50, 136° for BFN 75 and 142° for BFN 100.

The ceramics powder milled high – energetic method has a positive impact on the value of dielectric losses for the BFN ceramic samples (Fig. 4b). The value of tanδ is lower in comparison with the one obtained for ceramics prepared by classic ceramic technology [19]. The increase of milling time caused decrease of the value of dielectric losses. The rapid increase of the dielectric losses above 220 °C is associated with the increase of electrical conductivity at high temperatures.

Graphs of ln$\sigma_{DC}(1/T)$ for BFN ceramic samples show that for all the studied samples changes the nature of the electrical conductivity is similar (Fig. 6). In the graphs there are characteristic inflection points (two areas) where there is a change in the activation energy. Change the value of the activation energy E_{Act} visible in the phase transition (area II) confirms the ferroelectric properties of the obtained material BFN. Activation energies calculated

according to the Arrhenius law:

$$\sigma_{DC} = \sigma_0 e^{-\frac{E_{\mathrm{Act}}}{k_B T}} \quad (1)$$

where: k_B – Boltzmann constant, E_{Act} – activation energy, T – absolute temperature.

Like most materials with perovskite structure also for the BFN ceramics there is an increase in value of activation energy E_{Act} in a paraelectric phase (Tab. 1). The value of the activation energy for ceramic samples does not change significantly from the high-energy milling time. The lowest conductivity shows the BFN 100 sample, milled the longest.

The temperature dependence of relaxation time can be expressed as $\tau = \tau_0 \exp(E_{\mathrm{Act}}/kT)$ from impedance studies, where: E_{Act} is the activation energy for relaxation processes and the pre-factor t_0 represents the relaxation time at infinite temperature (Tab. 1). The relaxation time is the smallest for intermediate high-energy milling times (for 50 h and 75 h) and the largest for the longest mechanical activation time (100 h).

4 Conclusions

During the high-energy milling of BFN powders, prereaction between the BFN components has been observed and among intermediate phase the perovskite one has been formed. Larger number of defects, occurred during prolonged milling, facilitates the diffusive processes in the powder. With the increase of the high-energy milling time, due to the high degree of fragmentation and large number of defects, the material becomes more amorphous. The final and total synthesis is achieved during additional annealing e.g. during sintering of BFN ceramic samples.

The studies of influence of the high-energy milling time on the dielectric properties and DC electrical conductivity. BFN ceramics, shown that the optimal mechanical activation times are in the area from 50 h to 75 h. Samples obtained under these technological conditions exhibit optimum of the parameters in the analyzed group of the BFN ceramic samples.

In the BFN material, high dielectric values are accompanied by a significant loss dielectric. The use of mechanical activation in the technological process of ceramic preparation reduces the dielectric losses in comparison with BFN ceramics obtained by classic methods.

References

1. R. Skulski, P. Wawrzała, J. Korzekwa, M. Szymonik, Arch. Metall. Mater. **54**, 4 935 (2009)
2. Z. Surowiak, D. Bochenek, Arch. Acoust. **33**, 243 (2008)
3. J.F. Scott, J. Mater. Chem. **22**, 4567 (2012)
4. P. Wawrzała, J. Korzekwa, Ferroelectrics **446**, 91 (2013)
5. EU-Directive 2002/95/EC, Restriction of the Use of Certain Hazardous Substances in Electrical and Electronic Equipment (RoHS), Official Journal of the European Union **46**, L37, 19 (2003)
6. EU-Directive 2002/96/EC, Waste Electrical and Electronic Equipment (WEEE), Official Journal of the European Union, **46**, L37, 24 (2003)
7. *Lead-Free Piezoelectrics*, edited by S. Priya, S. Nahm (Springer, New York, 2012)
8. D. Bochenek, Z. Surowiak, J. Poltierova-Vejpravova, J. Alloys Compd. **487**, 576 (2009)
9. D. Bochenek, P. Niemiec, A. Chrobak, G. Ziółkowski, A. Błachowski, Mater. Charact. **87**, 36 (2014)
10. S. Saha, T.P. Sinha, J. Phys.: Condens. Matter **14**, 249 (2002)
11. I.P. Raevski, S.A. Prosandeev, A.S. Bogatin, M.A. Malitskay, L. Jastrabik, J. Appl. Phys. **93**, 4130 (2003)
12. I. Szafraniak, M. Połomska, B. Hilczer, A. Pietraszko, L. Kępiński, J. Eur. Ceram. Soc. **27**, 4399 (2007)
13. T. Rojac, A. Benčan, M. Kosec, J. Am. Ceram. Soc. **93**, 1619 (2010)
14. I. Szafraniak-Wiza, W. Bednarski, S. Waplak, B. Hilczer, A. Pietraszko, L. Kępiński, J. Nanosci. Nanotechnol. **9**, 3246 (2009)
15. The Inorganic Crystal Structure database (ICSD), code 43622
16. S. Ke, H. Fan, H. Huang, J. Electroceram. **22**, 252 (2009)
17. S. Eitssayeam, U. Intatha, K. Pengpat, G. Rujijanagul, K.J.D. MacKenzie, T. Tunkasiri, Curr. Appl. Phys. **9**, 993 (2009)
18. Chao-Yu Chung, Yen-Hwei Chang, Guo-Ju Chen, Yin-Lai Chai, J. Cryst. Growth **284**, 100 (2005)
19. S. Eitssayeam, U. Intatha, K. Pengpat, T. Tunkasiri, Curr. Appl. Phys. **6**, 316 (2006)